MOLECULAR AND CELLULAR BIOLOGY, July 2006, p. 4958–4969 Vol. 26, No. 13
0270-7306/06/$08.00+0 doi:10.1128/MCB.00160-06

Distinct Functional Domains of Ubc9 Dictate Cell Survival and Resistance to Genotoxic Stress

Robert C. A. M. van Waardenburg,[1] David M. Duda,[2] Cynthia S. Lancaster,[1] Brenda A. Schulman,[2,3] and Mary-Ann Bjornsti[1]*

Department of Molecular Pharmacology,[1] Howard Hughes Medical Institute,[3] and Department of Structural Biology and Genetics/Tumor Cell Biology,[2] St. Jude Children's Research Hospital, 332 N. Lauderdale, Memphis, Tennessee 38105

Received 27 January 2006/Accepted 29 March 2006

Covalent modification with SUMO alters protein function, intracellular localization, or protein-protein interactions. Target recognition is determined, in part, by the SUMO E2 enzyme, Ubc9, while Siz/Pias E3 ligases may facilitate select interactions by acting as substrate adaptors. A yeast conditional Ubc9P$_{123}$L mutant was viable at 36°C yet exhibited enhanced sensitivity to DNA damage. To define functional domains in Ubc9 that dictate cellular responses to genotoxic stress versus those necessary for cell viability, a 1.75-Å structure of yeast Ubc9 that demonstrated considerable conservation of backbone architecture with human Ubc9 was solved. Nevertheless, differences in side chain geometry/charge guided the design of human/yeast chimeras, where swapping domains implicated in (i) binding residues within substrates that flank canonical SUMOylation sites, (ii) interactions with the RanBP2 E3 ligase, and (iii) binding of the heterodimeric E1 and SUMO had distinct effects on cell growth and resistance to DNA-damaging agents. Our findings establish a functional interaction between N-terminal and substrate-binding domains of Ubc9 and distinguish the activities of E3 ligases Siz1 and Siz2 in regulating cellular responses to genotoxic stress.

The covalent attachment of ubiquitin (Ub) or Ub-like proteins (Ubls) to lysine residues alters target protein function in a variety of biological processes (6, 10, 12, 16). As with other Ubls, the *s*mall *u*biquitin-related *mo*difier SUMO is reversibly conjugated to substrate proteins via a conserved cascade of enzymes. In *Saccharomyces cerevisiae*, SUMO is encoded by an essential gene, *SMT3*, while there are four human SUMO paralogs (12, 16). For ease of presentation, SUMO/Smt3 will collectively be referred to as SUMO, with discussions of yeast Smt3 restricted to specific examples. SUMO, like Ub, is expressed as an inactive precursor (6, 12, 16). Proteolytic processing by SUMO-specific proteases, such as yeast Ulp1, yields the mature di-Gly C terminus. A heterodimeric E1 enzyme (yeast Aos1/Uba2) initiates conjugation by adenylating SUMO, followed by the formation of a covalent thioester E1-SUMO intermediate. SUMO is then transferred to the catalytic cysteine of the E2, Ubc9, which alone or in concert with an E3 ligase catalyzes the formation of an isopeptide linkage between the C-terminal carboxyl group of SUMO and the ε-amino group of the substrate lysine residue. Isopeptidases catalyze de-SUMOylation, and thus a balance of Ubc9 conjugation and isopeptidase activities modulate steady-state levels of SUMO conjugates.

In budding yeast and mammalian cells, Ubc9 is the sole SUMO-conjugating enzyme and is essential for cell viability (13, 25, 38). In contrast to Ub conjugation, where substrate specificity is dictated by E3 ligases, SUMO target recognition is determined, in part, by the E2 Ubc9. Structural and biochemical data indicate selective binding of a consensus ΨKX(D/E) motif by Ubc9, where Ψ is a hydrophobic residue, X is any amino acid, and K is the lysine modified with SUMO (2, 17, 36). However, the relative simplicity of this pathway belies the complexity of protein targets modified by SUMO. The limited substrate specificity imparted by Ubc9 interactions with ΨKXE residues is insufficient to account for the increasing number of proteins modified by SUMO and the modification of proteins at nonconsensus SUMO sites (5, 11, 24, 28, 37, 43, 44, 48). Ubc9-target interactions may also be facilitated by E3 ligases, such as the Siz/PIAS family, RanBP2, and Polycomb Pc2 protein (12, 16, 24, 31). Siz/PIAS E3 ligases appear to act as substrate adaptors. In contrast, recent structural studies suggest that the IR1-M E3 ligase domain of RanBP2 binds SUMO and Ubc9 to optimize the orientation of the SUMO-Ubc9 thioester, thereby enhancing conjugation (35, 40). Thus, E3 ligases may function as chaperones to facilitate SUMO conjugation in the absence of direct substrate interactions. However, whether Ubc9 contains additional determinants of substrate specificity and what role E3 ligases play in the recognition of select targets remain unclear.

Covalent modification with SUMO can alter target protein subcellular localization, activity, stability, or protein-protein interactions, thereby affecting various processes, including gene transcription, apoptosis, cell cycle progression, chromatin organization, and DNA repair (6, 10, 12, 16). Proteomic approaches have defined a large number of SUMO substrates in yeast and human cells (5, 11, 24, 28, 37, 43, 44, 48). Yet, it appears that only a small percentage of a given protein is covalently modified by SUMO at any time. Thus, the functional analysis of SUMO-modified substrates is complicated, as persistent alterations in protein function may be induced by relatively transient cycles of SUMO modification.

Eukaryotic cell sensitivity to DNA-damaging agents is also affected by SUMO conjugation. Postreplicative DNA repair is regulated, in part, by the addition of mono-Ub or poly-Ub to

* Corresponding author. Mailing address: Dept. of Molecular Pharmacology, St. Jude Children's Research Hospital, 332 N. Lauderdale, Memphis, TN 38105. Phone: (901) 495-2315. Fax: (901) 495-4293. E-mail: mary-ann.bjornsti@stjude.org.

TABLE 1. Yeast plasmids

Plasmid[a]	Characteristics	Reference
YCpSc · U	A 0.5-kb DNA fragment bearing the yeast *TOP1* promoter (p*TOP1*) was PCR amplified from yeast genomic DNA and ligated into HindIII-BamHI sites of pRS416[b]	This study
YCpSctop1T722A · U	A 2.9-kb BamHI-XbaI fragment excised from YCpGAL1top1T722A (23) was ligated into YCpSc · U	This study
YCpGPD · U	The 0.7-kb yeast *GPD* promoter, PCR amplified from yeast genomic DNA, was ligated into HindIII-BamHI sites of pRS416[b]	This study
YCpGPDyUBC9 · U	A 0.6-kb fragment, PCR amplified from YCpUBC9 · U (15), was ligated into the BamHI-NotI sites of YCpGPD · U[b]	This study
YCpSc · H	The *TOP1* promoter, excised from YCpSc · U, was cloned into HindIII-BamHI sites of pRS413	This study
YCpSctop1T722A · H	*top1T722A HIS3 CEN6 ARSH4*; a 3.5-kb XhoI-NotI fragment, excised from YCpSctop1722A · U, was ligated into the same sites in pRS413	This study
YCpUBC9 · L	A 2.2-kb BamHI-NotI genomic fragment from YCpUBC9 · U was ligated into pRS415	This study
YCpGPD · L	The *GPD* promoter, excised from YCpGPD · U, was ligated into HindIII-BamHI sites of pRS415	This study
YCpGPDhUBC9 · L	Human UBC9 cDNA sequences, PCR amplified from pooled human cDNA and cloned into pGEX4T3, were PCR amplified and ligated into the BamHI-NotI sites of YCpGPD · L[b]	This study
YCpGPDhUBC9^{myc} · L	A C-terminal Myc-tagged hUbc9, generated by PCR followed by cloning into BamHI-NotI sites of YCpGPD · L[b]	This study
YCpGAL1 · U	A 0.8-kb fragment containing the yeast *GAL1* promoter (pGAL1) was PCR amplified from yeast genomic DNA and inserted into the HindIII-BamHI sites of pRS416	This study
YCpGAL1hUBC9 · U	hUBC9 cDNA ligated into the BamHI-NotI sites of YCpGAL1 · U	This study
YEp24-PL	Modified YEp24 vector with multiple cloning site of pBluescript II	34
YEpSIZ1 · U	A 4.3-kb SmaI-SacI genomic fragment containing *SIZ1* was excised from a YEp-FY250 genomic DNA library clone (C. S. Lancaster and M.-A. Bjornsti unpublished results) and inserted into YEp24-PL	This study
YEpSIZ1 · T, · L, · U	The SmaI-SacI fragment from YEpSIZ1 · U inserted into pRS424, pRS425, or pRS426	This study
YEpSIZ2 · L, · U	A 2.6-kb XhoI-NotI genomic fragment containing *SIZ2* plus 500 bp 5′ of ATG was PCR amplified from genomic DNA, and cloned into pRS425 or pRS426, and confirmed by sequencing[b]	This study
YEpUBC9 · L	The BamHI-NotI genomic fragment from YCpUBC9 inserted into pRS425	This study
YEpGAL1 · L	pGAL1 inserted into the HindIII-BamHI sites of pRS425	This study
YEpGAL1yUBC9 · L	A yUBC9 PCR product was inserted into BamHI-NotI sites of YEpGAL1 · L[b]	This study
YEpGAL1yUBC9^{myc} · L	A C-terminal Myc epitope-tagged yUBC9 construct was PCR amplified and inserted into the BamHI-NotI sites of YEpGAL1 · L[b]	This study
YEpGAL1hUBC9 · L	hUBC9 cDNA sequences ligated into BamHI-NotI sites of YEpGAL1 · L	This study
YEpGAL1hUBC9^{myc} · L	A hUBC9^{myc} PCR product was ligated into BamHI-NotI sites of YEpGAL1 · L	This study
YEpGAL1hUBC9^{flag} · L	A C-terminal Flag-tagged hUBC9 construct was PCR amplified and inserted into the BamHI-NotI sites of YEpGAL1 · L[b]	This study
YEpGAL1hubc9P123L · L	A Pro123(CCA)-to-Leu(CTA) mutation was generated by site-directed mutagenesis of YEpGAL1hUBC9 · L	This study

[a] A U, L, H, or T suffix indicates a *URA3*, *LEU2*, *HIS3*, or *TRP1* marker, respectively.
[b] Primer sequences are available upon request.

K_{164} in proliferating cell nuclear antigen (PCNA) in response to DNA damage (30, 42). Surprisingly, Ubc9 conjugates SUMO to the same residue in PCNA, thereby implicating distinct modifications in response to different replication stresses. Although *UBC9* is essential for cell viability, conditional yeast *ubc9* mutants exhibit increased sensitivity to DNA-damaging agents (15, 22). We reported the isolation of the *ubc9P$_{123}$L* mutant in a yeast genetic screen for conditional mutants exhibiting enhanced sensitivity to DNA lesions induced by drugs that target DNA topoisomerase I (Top1) (15). At the nonpermissive temperature, 36°C, global SUMO conjugates were severely suppressed in cells expressing Ubc9P$_{123}$L, yet cell viability was retained. Relative to wild-type *UBC9* strains, *ubc9P$_{123}$L* cells exhibited enhanced sensitivity to a wide range of DNA-damaging agents (including drugs that target Top1, hydroxyurea [HU], the alkylating agent methyl methanesulfonate [MMS], and UV light) but not to other environmental stress. Although Top1 is modified by SUMO, the enhanced sensitivity of *ubc9P$_{123}$L* cells to DNA damage was not dependent on Top1 SUMO conjugation or expression. Rather, a lower threshold of select SUMO-target conjugates was required to maintain cell viability in the absence of genotoxic stress. This premise was further supported by the observation that the viability, but not the HU resistance, of cells deleted for the Ulp2 SUMO-isopeptidase was restored by the reduced activity of Ubc9P$_{123}$L at 36°C (15).

In order to define functional domains in Ubc9 that dictate cellular responses to DNA-damaging agents versus those necessary for cell viability, we took advantage of the conservation between human Ubc9 and yeast Ubc9 (hUbc9 and yUbc9, respectively) to assess the consequences of subtle structural alterations in SUMO E2 enzyme activity. We solved the structure of yUbc9 and, based on comparisons with crystal structures of hUbc9 (41), constructed a series of chimeric enzymes to define the functions of specific amino acid residues in regulating enzyme activity in vivo. Here we report that differences in the geometries of divergent side chain residues within protein domains implicated in (i) binding of substrate residues flanking the canonical SUMO site, (ii) interaction with the RanBP2 E3 ligase, and (iii) binding of the heterodimeric E1 and Smt3 have distinct effects on cell growth and resistance to DNA-damaging agents.

TABLE 2. Human-yeast UBC9 chimeras

Plasmid[a]	Description[b]
YEpGAL1h123yUBC9 · L	A human-yeast UBC9 chimera, PCR amplified from YCpUBC9, was cotransformed into EKY3 cells with NotI-linearized YCpGAL1hUBC9 · U; sequencing confirmed the chimera junction at residue 123 in plasmids recovered from uracil prototrophs, and the h123yUBC9 chimera was then inserted into the BamHI-NotI sites of YEpGAL1 · L
YEpGAL1h143yUBC9 · L	As above, a h143yUBC9 chimera was generated by PCR; the h143y chimera in recombinant *URA3* plasmids was confirmed by sequencing
YEpGAL1h123y143hUBC9 · L	As above, a human-yeast-human UBC9 chimera was generated by PCR, followed by cotransformation with NotI-linearized YEpGAL1h123yUBC9 · L; the h123y143h chimera in recombinant *URA3* plasmids was confirmed by sequencing.
YEpGAL1y123hUBC9 · L	As above, a yeast-human UBC9 chimera, PCR amplified from YCpGAL1hUBC9 · U, was cotransformed with NotI-linearized YCpUBC9; sequencing of plasmids recovered from uracil prototrophs confirmed the y123h chimera, which was then excised and ligated into YEpGAL1 · L
YEpGAL1y143hUBC9 · L	As above, a y143hUBC9 chimera was generated by PCR and confirmed by sequencing
YEpGAL1h22yUBC9 · L	A human-yeast UBC9 chimera was PCR amplified and cotransformed into EKY3 cells with BamHI-linearized YCpGAL1yUBC9 · U; sequencing confirmed the chimera junction at residue 22 in plasmids recovered from uracil prototrophs, and the h22yUBC9 chimera was then inserted into the BamHI-NotI sites of YEpGAL1 · L
YEpGAL1y22hUBC9 · L	As above, a y22hUBC9 chimera was generated by PCR and confirmed by sequencing
YEpGAL1h38yUBC9 · L	As above, a h38yUBC9 chimera was generated by PCR and confirmed by sequencing
YEpGAL1y38hUBC9 · L	As above, a y38hUBC9 chimera was generated by PCR and confirmed by sequencing
YEpGAL1h42yUBC9 · L	As above, a h42yUBC9 chimera was generated by PCR and confirmed by sequencing
YEpGAL1y42hUBC9 · L	As above, a y42hUBC9 chimera was generated by PCR and confirmed by sequencing
YEpGAL1y22h123y143hUBC9 · L	A y22hUBC9 chimera was generated in YEpGAL1h123y143hUBC9 · L by PCR and confirmed by sequencing
YEpGAL1y38h123y143hUBC9 · L	A y38hUBC9 chimera was generated in YEpGAL1h123y143hUBC9 · L by PCR and confirmed by sequencing

[a] The corresponding YCp series of vectors were also generated in pRS415.
[b] Primer sequences are available upon request.

MATERIALS AND METHODS

Chemicals, yeast strains, and plasmids. Camptothecin (CPT) was purchased from Sigma Chemical Co. (St. Louis, MO). Stock solutions of CPT (4 mg/ml in dimethyl sulfoxide) were stored at −20°C. 5-Fluoroorotic acid and HU were from U.S. Biological (Swampscott, NY).

Isogenic *S. cerevisiae* strains FY250 (*MATα ura3-52 his3Δ200 leu2Δ1 trp1Δ63*), EKY3 (FY250 *top1Δ::TRP1*), RRY82 (EKY3 *ubc9-10*), HJY13 (FY250 *ubc9-10*), and PTY30 (EKY3 *ubc9Δ:: his*$^+$, YCpUBC9) were described previously (15). Yeast cells were transformed and cultured using standard methods.

Yeast plasmids are listed in Table 1. The Pro_{123}-to-Leu mutation in h*Ubc9*P_{123}*L* was generated in YCpSchUBC9 by using the QuikChange site-directed mutagenesis kit (Stratagene). Yeast-human *UBC9* chimeras were generated by homologous recombination (29) of PCR-generated chimeric junctions (Table 2).

Cell viability assays. Exponentially growing cultures of cells (A_{595} = 0.3) transformed with the indicated plasmids were serially 10-fold diluted, spotted onto the appropriate selective medium supplemented with dextrose or galactose, and incubated at 26°C or 36°C. To assay cell sensitivity to HU or MMS, plates were supplemented with 5 mg/ml HU or 0.0125% MMS, respectively. For CPT sensitivity, the medium was supplemented with 25 mM HEPES (pH 7.2) and 0 or 5 μg/ml CPT in a final 0.125% dimethyl sulfoxide.

Antibodies and immunoblots. Ubc9 antibodies (A645 from Boston Biochem) recognize yUbc9 and hUbc9. Rat α-tubulin antibodies were from Accurate Chemical and Scientific Corp (Westbury, NY), anti-Myc antibodies (clone 9E10) were from Roche Diagnostics Corp. (Indianapolis, IN), anti-Flag M2 antibodies were from Sigma, and anti-Smt3 antibodies were provided by E. S. Johnson (Thomas Jefferson University) or raised against purified Smt3 in rabbits. Anti-yUbc9-specific antibodies were described previously (15). Anti-hUbc9 specific antibodies were raised against residues 59 to 71 in rabbits and affinity purified on peptide-coupled Sepharose 4B using standard techniques as described previously (15).

To assess the levels of yUbc9, hUbc9, and Smt3 conjugates, galactose-induced cultures were grown for 6 h at 26°C or 36°C and NaOH-trichloroacetic acid extracts were prepared as described previously (15). Proteins were resolved in 12% or 4 to 12% Bis-Tris polyacrylamide gels with MOPS (morpholinepropanesulfonic acid) running buffer (NuPAGE; Invitrogen) and blotted onto activated polyvinylidene difluoride membranes (Perkin-Elmer, LifeScience). Ubc9 proteins or Smt3 conjugates were visualized by immunostaining and chemiluminescence. Immunostaining with α-tubulin served as a loading control.

In vitro SUMO conjugation assays. The heterodimeric yE1 (yAos1/Uba2), yUbc9, and a truncated version of Smt3, which terminates at G_{98} to represent the mature form, were expressed in BL21(DE3) cells (Novagen) and purified as described previously (1). A cDNA clone expressing full-length hUbc9 was obtained by PCR amplification of human cDNA (Invitrogen) and cloned into pGEX4T3. Following expression in BL21(DE3) cells, hUbc9 was purified by glutathione affinity chromatography as described previously (1). The N-terminal glutathione *S*-transferase tag was removed by overnight treatment with thrombin at 4°C, and Ubc9 proteins were purified by ion-exchange chromatography using a Resource Q column pressured by an AKTA fast protein liquid chromatography system (GE Healthcare) and by size exclusion chromatography using an SD200 column (GE Healthcare), concentrated by ultrafiltration, frozen in liquid nitrogen, and stored at −80°C.

Formation of yUbc9-Smt3, hUbc9-Smt3, and Smt3-Smt3 conjugates was assessed following incubation of 10 μg of hUbc9 or yUbc9, 40 μg of Smt3, and either 0.1 μg (1×), 1 μg (10×), or 10 μg (100×) of Aos1/Uba2 in 30 to 50 mM Tris (pH 7.5), 100 mM NaCl, 10 mM $MgCl_2$, and 4 mM ATP in a volume of 35 to 50 μl. Reaction mixtures were incubated at room temperature for 0, 15, or 60 min and terminated with sodium dodecyl sulfate sample buffer lacking dithiothreitol (DTT). The samples were equally divided, with half treated with 100 mM DTT prior to boiling. Reaction products were resolved in 4 to 12% Bis-Tris polyacrylamide gels (Novagen) in MES (morpholineethanesulfonic acid) buffer and visualized by Coomassie or SYPRO-Ruby staining. The identities of specific bands, previously defined by matrix-assisted laser desorption ionization–time-of-flight mass spectrometry (1), were confirmed by immunostaining.

Crystallization, data collection, and structure determination. Initial crystals of yUbc9 were obtained in 21% polyethylene glycol 4000 (PEG 4000), 0.1 M MES (pH 6.0), 0.1 M NaBr, and 5 mM DTT by using the hanging-drop vapor diffusion method at 18°C. High-quality crystals for X-ray diffraction were grown by microseeding into 18% PEG 6000, 0.1 M HEPES (pH 7.5), 0.1 M NaBr, and 5 mM DTT. The crystals belong to the P21 space group with unit cell dimensions a = 59.3 Å, b = 60.1 Å, c = 95.3 Å, and β = 105.0° and four monomers per asymmetric unit. Crystals were flash frozen in 21% PEG 6000, 50 mM HEPES (pH 7.5), 0.1 M NaBr, 5 mM DTT, and 30% glycerol prior to data collection at

TABLE 3. Summary of diffraction data

Parameter (unit)	Value[a]
Wavelength (Å)	1.1000
Resolution (Å)	1.75
No. of:	
Observations	1,502,049
Unique reflections	65,526
Completeness (%)	99.5 (98.9)
R_{merge}[b] (%)	4.8 (40.2)
Avg $I/\sigma I$	
Overall	58.7
Last shell	15.9

[a] Values in parentheses are for the last shell.
[b] $R_{merge} = \Sigma I(\kappa) - \langle I \rangle / \Sigma I(\kappa)$, where $I(\kappa)$ is the value of the κth measurement of the intensity of a reflection, $\langle I \rangle$ is the mean value of the intensity of that reflection, and the summation is of all the measurements.

TABLE 4. Refinement statistics and model quality

Parameter (unit)	Value[a]
Resolution (Å)	25-1.75
No. of:	
Reflections (working set)	61,884
Reflections (test set)	3,311
Total atoms	5,493 (31.6)
Protein atoms	5,022 (27.9)
Solvent atoms	471 (35.3)
R factor (%)	22.13
R_{free} (%)	24.51
Ramachandran plot	
Core and additionally allowed regions (%)	99.2
Generously allowed regions (%)	0.8
Disallowed regions (%)	0.0
RMS deviation from ideal geometry	
Bond lengths (Å)	0.005
Bond angles (°)	1.327

[a] Values in parentheses are B factors (Å^2).

the National Synchrotron Light Source beamline X25. Data were collected from a single crystal to 1.75-Å resolution with 1,502,049 total reflections and 65,526 unique reflections. The data were indexed with HKL2000 and scaled with SCALEPACK (27) to a final R_{merge} of 4.8% and overall completeness of 99.5%. Phases were obtained by molecular replacement using polyalanine hUbc9 (PDB accession no. 1U9A [41]) as the search model in AMORE (26). The model was refined using CNS version 1.1 (3), with real-space model refinement and visualization performed in O version 9.0 (19). The refinement proceeded until convergence with an *R* factor of 22.1% and an R_{free} of 24.5%. The average B factor for 5,022 protein atoms was 27.9 Å^2, and that for 471 solvent atoms located in the asymmetric unit was 35.3Å^2. The fraction of residues in the core and additionally allowed regions of the Ramachandran plot was 99.2%, with no residues in the disallowed region, as determined by PROCHECK (20). A summary of diffraction data and refinement statistics are provided in Tables 3 and 4. All figures were made with PyMol (DeLano Scientific, San Carlos CA).

Protein structure accession number. The yeast Ubc9 structure was deposited in the PDB under accession number 2GJD.

RESULTS

Human Ubc9 function in yeast. We previously isolated temperature-sensitive yeast mutants with increased sensitivity to CPT, analogs of which constitute novel chemotherapeutics that selectively stabilize a covalent Top1-DNA intermediate (9, 15, 33). During S phase, the collision of advancing replication forks with CPT-Top1-DNA complexes produces irreversible DNA lesions that trigger cell cycle arrest and cell death (4, 8, 32). By using a self-poisoning *top1T$_{722}$A* mutant (23), which acts as a CPT mimetic, a *ubc9-10* mutant that was viable at 36°C in the absence of DNA damage but inviable in the presence of low levels of Top1 poisons was isolated (15). Here, substitution of Leu for Pro$_{123}$ (Ubc9P$_{123}$L) induced a reduction in global SUMO conjugates at 36°C, which sufficed to sustain cell viability yet enhanced cell sensitivity to a wide range of DNA-damaging agents.

Binding of substrates or E3 ligases to Ubc9 contributes to efficient SUMOylation; nevertheless, the role that the SUMO E2 itself plays in discriminating between substrates remains unclear. To address the role of Ubc9 residues in dictating cell survival and response to genotoxic stress, we exploited the similarities between yUbc9 and hUbc9 to ask how subtle alterations in structure would affect cell growth and survival. hUbc9 and yUbc9 are highly conserved proteins, exhibiting 56% identity (75% similarity) in amino acid sequence (Fig. 1A) (46). Using a plasmid shuffle in a *ubc9*Δ strain, hUbc9 complemented the essential function of yUbc9 when overexpressed from the *GAL1* promoter, albeit at a reduced rate of cell growth (Fig. 1B). However, the introduction of a C-terminal Myc epitope suppressed this slow-growth phenotype. Papillae in vector control and h*UBC9* patches result from recombination between *URA3* and *LEU2*-based vectors. Similar results were obtained when h*UBC9* was overexpressed from a strong constitutive promoter (*GPD*), obviating concerns about medium effects. In contrast, low constitutive expression of h*UBC9* failed to maintain *ubc9*Δ viability (data not shown).

To assess whether the deficit in hUbc9 activity in yeast represented differences in the formation of E2-thioester or substrate conjugates, purified yE1 (yAos1/Uba2), Smt3, and yUbc9 or hUbc9 were incubated in an in vitro SUMOylation assay. In the presence of ATP at 26°C, Smt3 and yUbc9 serve as substrates for Smt3 isopeptide linkages, while the extent of E2 thioester bond formation can be distinguished by treatment with DTT (1). A 100-fold excess of yE1 was required to achieve a time course of Ubc9-Smt3 and Smt3-Smt3 conjugates with hUbc9 that was comparable to that with yUbc9 (Fig. 1C). Moreover, the reduction in hUbc9-Smt3 conjugates in DTT-treated samples indicates that hUbc9 is not as efficient a substrate for SUMOylation as yUbc9 under these conditions. Thus, Ubc9 provides some determinants of E2 thioester transfer, which might be exploited to define differences in the biological function of yeast and human Ubc9.

We then asked if hUbc9 could complement the increased sensitivity of *ubc9-10* mutant cells to DNA-damaging agents. The slow-growth phenotype and enhanced HU or CPT sensitivity of *ubc9-10* cells at 36°C were suppressed by constitutive expression of wild-type yUbc9 and partially suppressed by leaky expression of the *GAL1-yUBC9* construct on dextrose (Fig. 2). In contrast, *GAL1*-promoted hUbc9 expression had

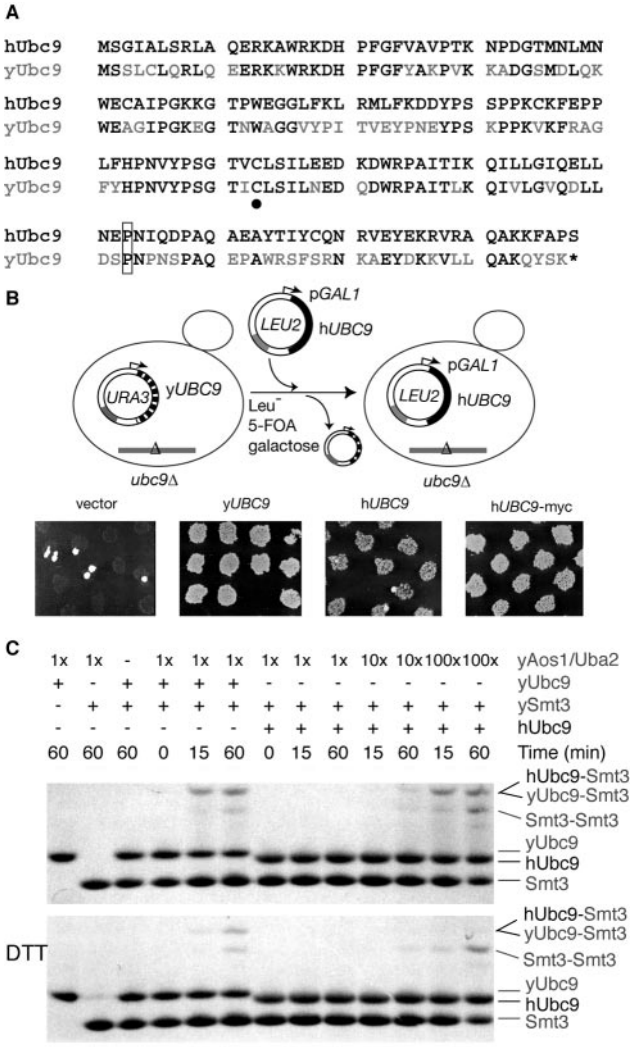

FIG. 1. Human *UBC9* complements yeast *ubc9*Δ. (A) Amino acid sequence alignment of human and yeast Ubc9. ●, active-site cysteine. The conserved Pro_{123} residue (mutated to Leu in yeast *ubc9-10*) is boxed. (B) In a plasmid shuttle assay, *ubc9*Δ cells transformed with a *LEU2* vector containing either y*UBC9*, *GAL1*-h*UBC9*, or -h*UBC9-myc* were patched onto selective medium and replica plated onto 5-fluoroorotic acid plates to cure cells of YCpyUBC9 · U. (C) Purified yUbc9 or hUbc9 was incubated in SUMOylation reaction mixtures supplemented with mature Smt3 and yE1 (yAos1/Uba2) at 26°C, with a 10- or 100-fold excess of yE1 as indicated. At 0, 15 or, 60 min, reactions were terminated with sodium dodecyl sulfate (with or without DTT), and Ubc9-Smt3 and Smt3-Smt3 conjugates were resolved by polyacrylamide gel electrophoresis and stained with Coomassie blue.

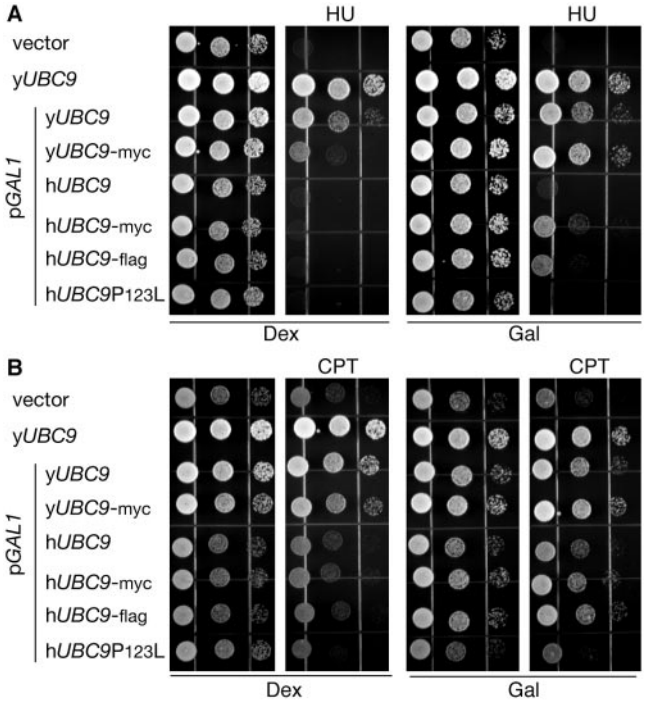

FIG. 2. hUbc9 does not restore cellular resistance to replication stress or CPT. *ubc9-10* cells, transformed with YEp vectors expressing y*UBC9* from its own promoter (y*UBC9*) or *UBC9* alleles from the *GAL1* promoter, were grown at 26°C, serially diluted, and spotted onto selective dextrose (Dex) or galactose (Gal) medium with or without HU (A) or onto selective Dex or Gal plates supplemented with HEPES, dimethyl sulfoxide, and CPT as indicated (B). Cell viability was assessed following incubation at 36°C.

little effect on *ubc9-10* cell sensitivity to HU or CPT, with only a slight increase in colony formation relative to the vector control. Thus, hUbc9 provides sufficient function to maintain yeast *ubc9*Δ cell viability yet apparently lacks determinants necessary to restore cellular resistance to genotoxic stress. Nevertheless, the phenotypic consequences of the $P_{123}L$ mutation were conserved: while overexpression of hUbc9$P_{123}L$ maintained *ubc9*Δ cell viability (data not shown), these cells were hypersensitive to HU and CPT (compare h*UBC9* with h*ubc9*P_{123}*L* in Fig. 2).

As in Fig. 1, the introduction of a C-terminal epitope facilitated hUbc9 function in yeast: expression of hUbc9-Myc or hUbc9-Flag partially restored cellular resistance to HU and CPT, relative to that observed with untagged hUbc9. The opposite effect was observed with yUbc9. Whereas overexpression of yUbc9 was slightly toxic (compare the slow-growth phenotype of *GAL1*-promoted y*UBC9* with the robust growth of cells expressing low constitutive levels of yUbc9), overexpression of yUbc9-Myc was less detrimental to cell growth and more efficient in suppressing *ubc9-10* cell sensitivity to HU and CPT (Fig. 2). Since comparable levels of yUbc9 and yUbc9-Myc proteins were expressed from the *GAL1* constructs (Fig. 3A), these data suggest that the C-terminal epitope suppressed the activity of yUbc9 in vivo, possibly through altered interactions with other components of the SUMO conjugation pathway.

hUbc9 was not detectable in immunoblots of cell extracts with pan-Ubc9- or hUbc9-specific antibodies (Fig. 3A and data not shown). However, as these antibodies efficiently recognized hUbc9 expressed in *Escherichia coli* (data not shown), we considered that modifications, such as N-terminal acetylation, might affect hUbc9 stability and/or immunodetection in yeast. Consistent with this, hUbc9 was detected in the supernatants from immunoprecipitation experiments (Fig. 3B). Moreover, mutation of Gly_3 in hUbc9 to the Ser residue found at the corresponding position in yUbc9 (Fig. 1A) allowed efficient immunodetection of hUbc9 (Fig. 3C). Although an indirect

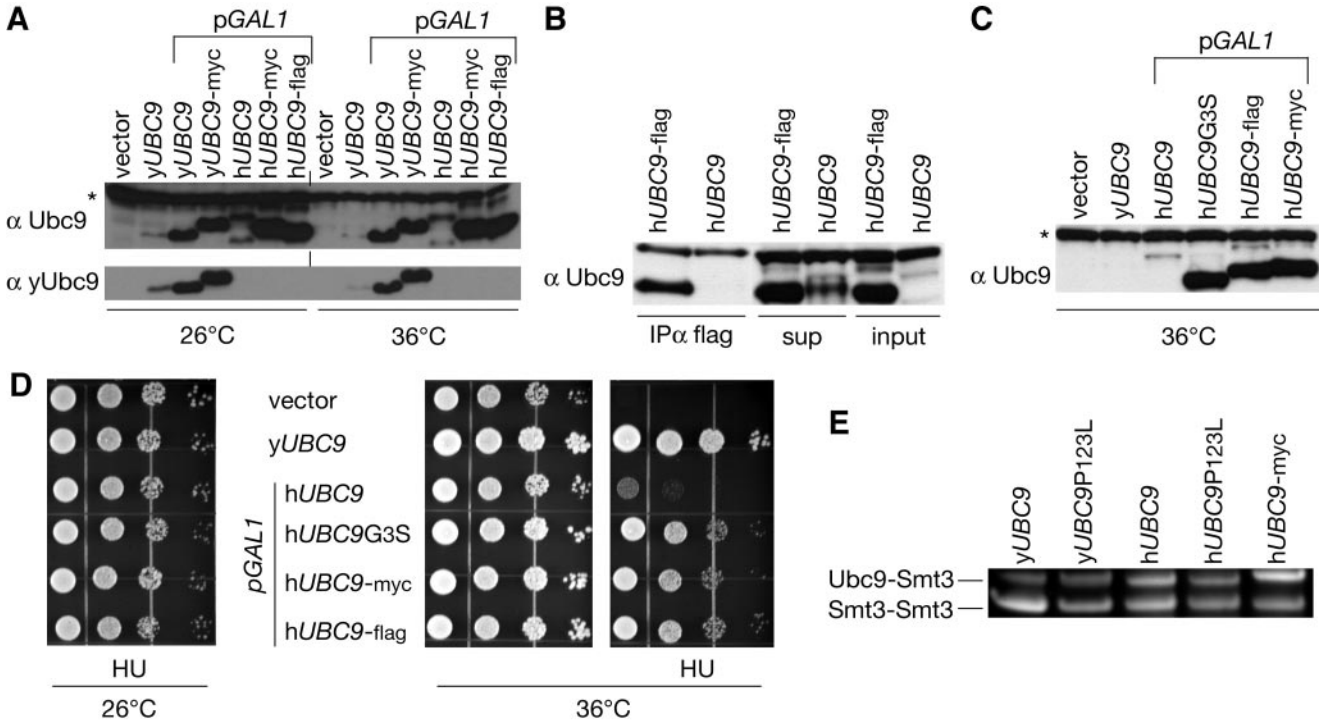

FIG. 3. Modification of N- or C-terminal residues affects hUbc9 protein detection in yeast. (A) *ubc9-10 top1*Δ cells (transformed with *UBC9* vectors shown in Fig. 2) were galactose induced at 26°C or 36°C, and cell extracts were immunoblotted with antibodies recognizing h/yUbc9 (α Ubc9) or specific for yUbc9 (α yUbc9). Equal protein loading, assessed by tubulin staining (not shown), was mirrored by the nonspecific band (*) in the α Ubc9 panel. (B) hUbc9-Flag or hUbc9, immunoprecipitated from cell extracts with anti-Flag antibodies, was immunoblotted with α Ubc9. Cell extracts (input), supernatant (sup), and immunoprecipitated protein (IPα flag) samples are shown. (C) As in panel A, Ubc9 proteins expressed at 36°C were detected in immunoblots of *ubc9-10 top1*Δ cell extracts stained with α Ubc9. (D) As in Fig. 2, dilutions of *ubc9-10 top1*Δ cells transformed with the indicated YEpGAL1-UBC9 vector were spotted onto selective galactose plates with or without HU and incubated at 26°C or 36°C. (E) The formation of isopeptide linkages between Smt3-Smt3 and Ubc9-Smt3 was assayed in vitro at 36°C, resolved by polyacrylamide gel electrophoresis in the presence of DTT, and stained with SYPRO-Ruby. hUbc9 proteins were incubated with a 100-fold excess of yE1.

effect of the G_3S substitution on the kinetics of hUbc9 degradation could not be excluded, this effect was not restricted to N-terminal residues, as C-terminally tagged proteins hUbc9-Myc and hUbc9-Flag were also efficiently recognized in immunoblots (Fig. 3A, B, and C). The levels of hUbc9G_3S and hUbc9-Flag/Myc proteins in galactose-induced cells were similar, and both the C-terminally tagged proteins and hUbc9G_3S partially restored *ubc9-10* cell resistance to HU at 36°C (Fig. 3D).

To determine if the phenotypic consequences of the $P_{123}L$ mutation or addition of a C-terminal epitope resulted from alterations in Ubc9 thioester transfer, the formation of Smt3 isopeptide linkages with Smt3 and Ubc9 was assessed in vitro. The extents of substrate SUMOylation catalyzed by yUbc9$P_{123}L$, hUbc9$P_{123}L$, and hUbc9-Myc were comparable to those obtained with relevant wild-type controls (Fig. 3E). Under these conditions (36°C, the nonpermissive temperature for *ubc9-10* cells), both Smt3 and Ubc9 were efficiently conjugated with Smt3. Moreover, as in Fig. 1C, reactions containing hUbc9 proteins were assayed with a 100-fold excess of yE1. Thus, mutation of Pro_{123} or a C-terminal tag had no detectable effect on Ubc9 catalysis in vitro. Rather, these findings prompted us to consider that alterations in substrate specificity, dictated by either differences in Ubc9 determinants or E3 ligase interactions, induced distinct cellular responses to genotoxic stress.

Structure determination of yeast Ubc9 and comparison with human Ubc9. The structure of yUbc9 (Fig. 4A) was determined from data collected at the National Synchrotron Light Source beamline X25 from a single crystal, with four monomers per asymmetric unit (Tables 3 and 4). Phases were obtained by molecular replacement using polyalanine hUbc9 (PDB accession no. 1U9A [41]) as a search model. The model was refined to 1.75 Å, with an R factor of 22.1 and R_{free} of 24.5. A least-squares fit of all four copies of yUbc9 in the asymmetric unit revealed a root mean square (RMS) deviation over all Cα atoms of 0.35 Å. As seen in Fig. 4B, further comparison of yUbc9 with hUbc9 (PDB accession no. 1A3S [41]) showed a considerable conservation of backbone structures, with an RMS deviation of 0.7 Å over all Cα atoms between the yeast and human forms.

Consistent with the similarities in yUbc9$P_{123}L$ and hUbc9$P_{123}L$ mutant phenotypes, P_{123} occupies the same position in both structures (Fig. 4). The recent cocrystal structure of hUbc9 in complex with SUMO-1 conjugated to RanGAP1 reveals hydrogen-bonding interactions between the E2 side chain of N_{85} with backbone atoms of E2 residue N_{124} and the C-terminal SUMO-1 G_{97} residue within the E2 active site (35). These residues are conserved in yUbc9 and Smt3. Also conserved are the majority of hUbc9 residues that interact with the consensus ΨKXE motif of RanGAP1 (2, 35), including Ubc9 residues

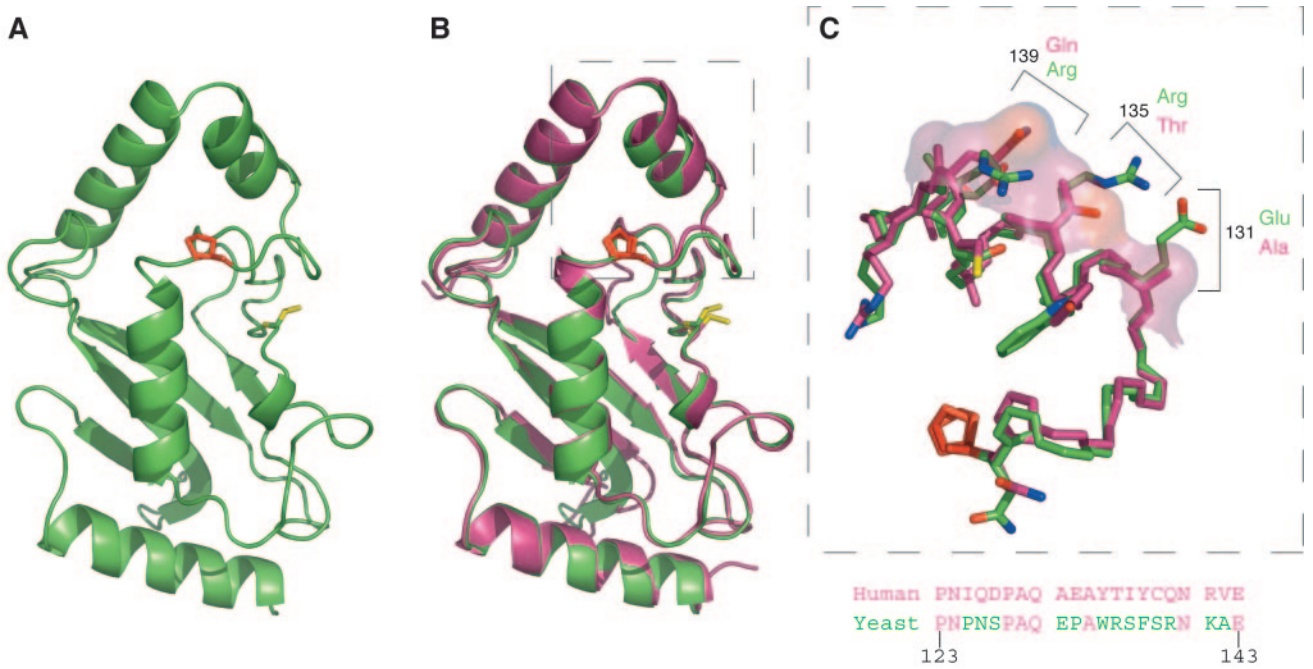

FIG. 4. Structural features of the substrate interaction domains of yeast and human Ubc9 proteins. (A) Ribbon diagram of yUbc9, resolved to 1.75 Å, with the active-site C_{93} in yellow and P_{123} in red. (B) Overlay of ribbon diagrams of yUbc9 (green) and hUbc9 (magenta) (PDB file 1A3S [41]). Two orientations of the active-site cysteine (yellow) were resolved in the yeast structures. (C) Close-up overlay of solid bond representations of the substrate interaction domain, residues 123 to 143 (boxed in panel B), with side chains shown for select residues and with transparent surface representation of human residues 131, 135, and 139.

K_{74}, Y_{87}, S_{89}, and T_{91}. Moreover, the flat surface immediately preceding residue 131, which interacts with the hydrophobic Ψ of the consensus motif, is superimposable in both structures (Fig. 4B [expanded in Fig. 4C]).

In hUbc9, residues 131 to 143 comprise helix C (Fig. 4B), which interacts with additional residues in RanGAP1 that lie outside the consensus ΨKXE site and have been implicated in select substrate binding (2, 35). Residues spanning the loop that precedes helix C include the P_{123} mutated in *ubc9-10* cells; however, as shown in Fig. 4C, 11 of the 13 residues comprising helix C are not conserved from yeast to human. Indeed, differences in residue side chains at positions 131 (Ala to Glu in yeast), 135 (Thr to Arg in yeast), and 139 (Gln to Arg in yeast) result in considerable alterations in surface charge and structure (Fig. 4C), which would clash with RanGAP1 residues in the SUMO-RanGAP1-Ubc9-RanBP2 structure (35) and disrupt critical hydrophobic interactions between A_{131} of hUbc9 and F_{564} of RanGAP1. Based on these considerations, we asked if such alterations in side chain geometry and charge would dictate differences in SUMO E2 activity in vivo.

C-terminal human/yeast Ubc9 chimeras. To address the functions of Ubc9 domains, homologous recombination (as described previously [29]) was used to generate reciprocal swaps of the C-terminal domains of yUbc9 and hUbc9, beginning at residue P_{123} or E_{143} (Fig. 5). In the designations, the first letter refers to the N-terminal sequence (h or y) and the number indicates the first residue of the C-terminal h or y Ubc9 component. The chimeras were expressed in *ubc9*Δ cells, using the plasmid shuffle shown in Fig. 1, to assess chimera E2 function in vivo. N-terminal proximal binding sites for yE1 and Smt3 were previously defined within yUbc9 (1). Thus, we reasoned that efficient E1-E2 interactions dictated by the yeast N terminus would obviate more subtle effects of substrate binding domains imparted by the human E2. Indeed, as seen with y_{123}hUbc9 or y_{143}hUbc9, expression of either chimera sufficed

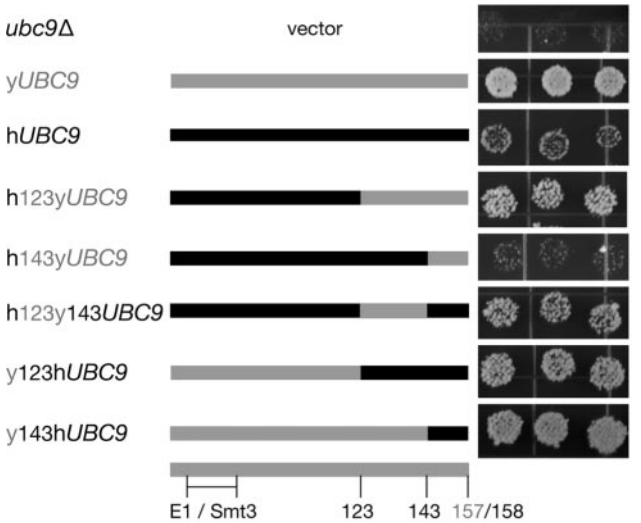

FIG. 5. Distinct yUbc9 domains enhance hUbc9 function in yeast *ubc9*Δ cells. Yeast-human (y/h) Ubc9 chimeras in *GAL1*-promoted vectors were introduced into *ubc9*Δ cells by plasmid shuffle (see Fig. 1B). The E1/Smt3 binding domain (1) and numbers referring to the first residue of the swapped domain are indicated in the yUbc9 scheme. yUbc9 sequences are in gray; hUbc9 sequences are in black. Photographs of independent strains, cured of YCpyUBC9 · U, were taken to emphasize differences in growth rates at 30°C.

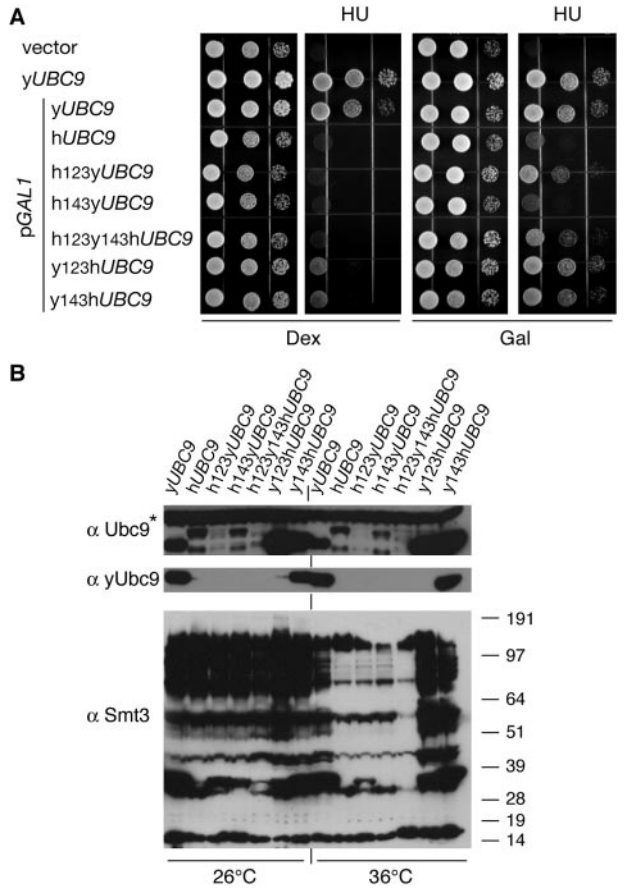

FIG. 6. y/hUbc9 chimeras fail to complement the defect in global SUMOylation. (A) As in Fig. 2, *ubc9-10 top1*Δ cells, transformed with YEp vectors containing y*UBC9*- or *GAL1*-promoted *UBC9* alleles, were spotted onto selective dextrose (Dex) or galactose (Gal) medium with or without HU and incubated at 36°C. (B) As in Fig. 3, galactose-induced cell extracts (26°C or 36°C) were probed with anti-Ubc9 (α Ubc9) antibodies or antibodies specific for yUbc9 or Smt3. Staining of the nonspecific band (*) in the α Ubc9 panel mirrored tubulin controls.

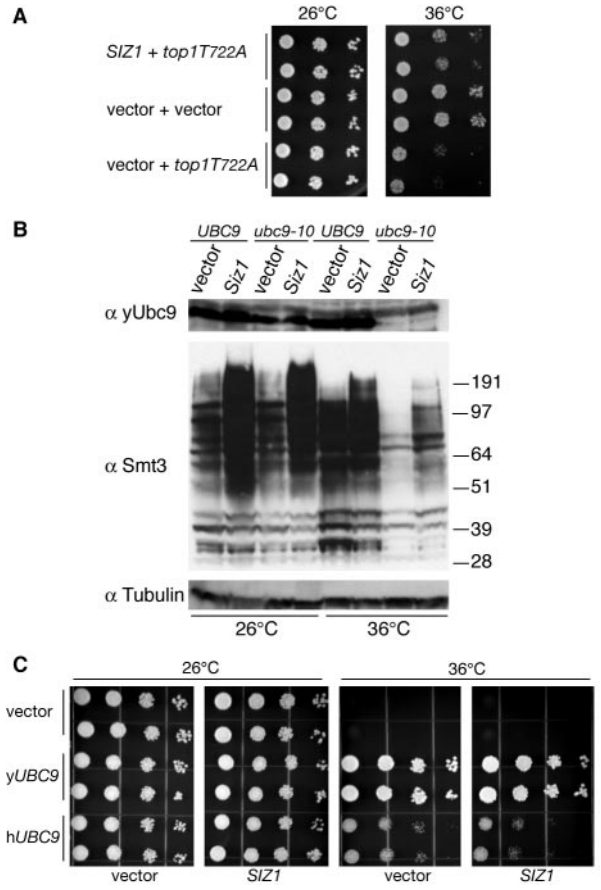

FIG. 7. Increased dosage of Siz1 E3 ligase restores *ubc9-10* cell resistance to Top1 poisons. (A) *ubc9-10 top1*Δ cells, cotransformed with YEpSIZ1 and YCpSctopT$_{722}$A or vector controls, were diluted, spotted onto selective medium, and incubated at 26°C or 36°C. (B) Extracts of wild-type *UBC9* or mutant *ubc9-10* strains, transformed with YEpSIZ1 or vector control, were immunoblotted with anti-yUbc9 (α yUbc9), α Smt3, or α tubulin antibodies. (C) *ubc9-10* cells, cotransformed with YEpSIZ1 and YEpyUBC9 or YEpGPDhUBC9, were spotted onto selective medium plus HU and incubated at 26°C or 36°C.

to maintain cell viability as well as wild-type yUbc9 (Fig. 5). Overexpression of hUbc9 also maintained cell viability, albeit with a slow-growth phenotype. The cell growth defect was suppressed by the introduction of the C-terminal yUbc9 domain, beginning at residue P_{123} in h_{123}yUbc9. However, this effect was not due to alterations of C-terminal sequences, as induced by the Myc tag (Fig. 1B), since defective cell growth was still seen with h_{143}yUbc9. Rather, the introduction of yeast residues 123 to 143, which span the $P_{123}N_{124}$ loop and helix C depicted in Fig. 4, enhanced hUbc9 function in maintaining yeast cell viability. Thus, in addition to N-terminal residues, two other determinants affect SUMO E2 function: alterations in the C terminus and residues spanning 123 to 143.

We then asked if the alterations in chimera h/yUbc9 activity, evident in *ubc9*Δ cells, also affected cell resistance to genotoxic stress. As seen in Fig. 6, the introduction of yeast residues 123 to 143 in $h_{123}y_{143}$hUbc9 dramatically increased *ubc9-10* cell resistance to HU at 36°C, relative to that observed with cells expressing wild-type hUbc9. However, none of these constructs restored the levels of global Smt3 conjugates detected in cells expressing yUbc9 (Fig. 6B). In contrast, the introduction of human C-terminal residues into yUbc9 abrogated the HU resistance induced by leaky expression on dextrose plates (compare y*UBC9* with the C-terminal chimeras, y_{123}h*UBC9* and y_{143}h*UBC9*). This effect was not due to differences in protein expression, as antibodies recognizing yeast residues 134 to 145 (anti-yUbc9) revealed comparable levels of wild-type yUbc9 and y_{143}hUbc9 (Fig. 6B). Moreover, similar levels of global Smt3 conjugates were detected in *ubc9-10* cells expressing wild-type yUbc9 or either of the y/h C-terminal chimeras. Thus, modified target selection, rather than the extent of global SUMOylation, appears to determine cellular resistance to DNA damage.

Ubc9 N-terminal residues and the Siz1 E3 ligase. Nuclear magnetic resonance and crystallographic data indicate extensive interactions between the RanBP2 E3 ligase and N-terminal residues of hUbc9, which overlaps the E1 binding site defined for yUbc9 (1, 35, 40). To distinguish between the effects of E1 versus E3 ligase interactions with Ubc9 on cell viability and sensitivity to DNA damage, we next investigated

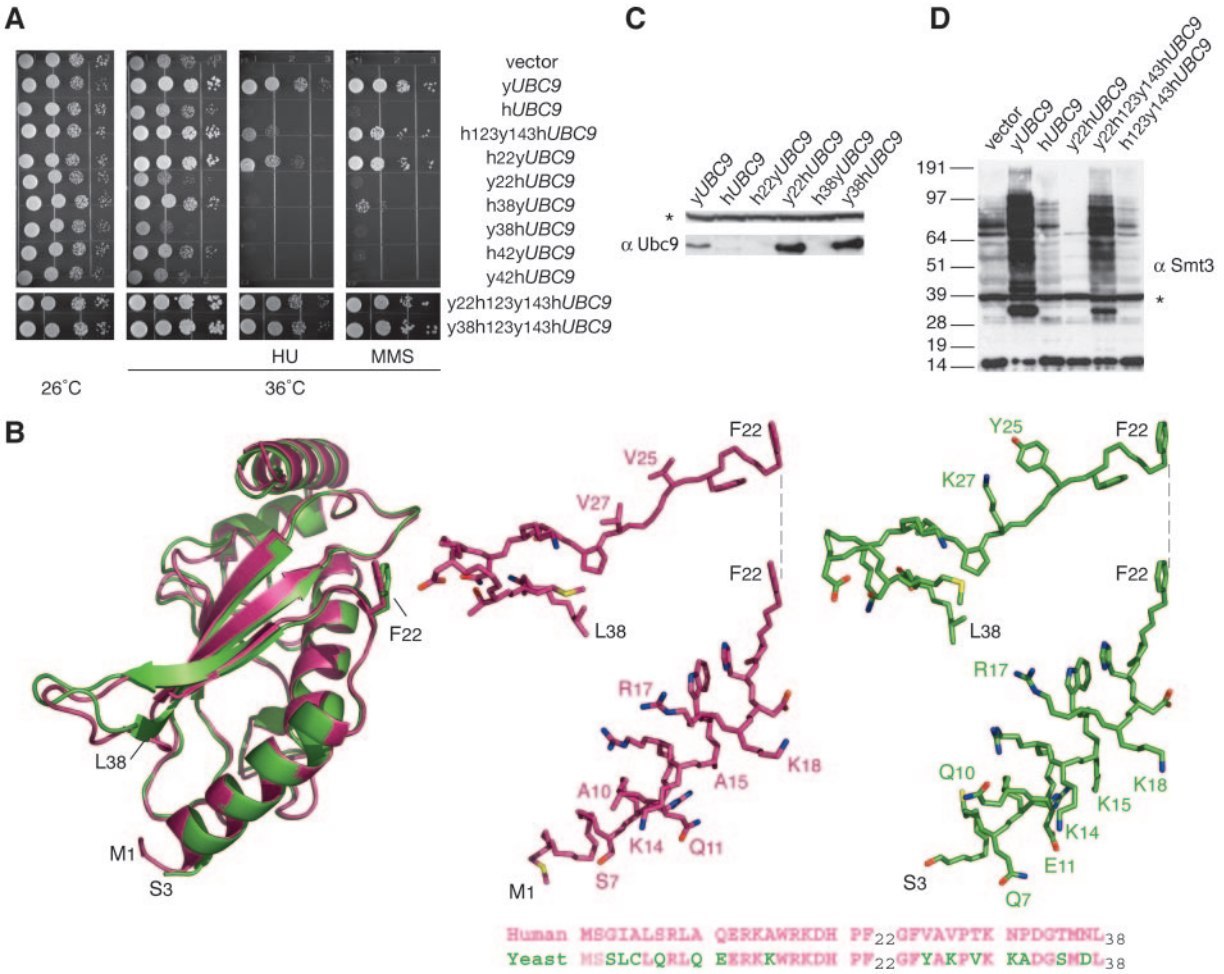

FIG. 8. Yeast Ubc9 N-terminal residues 22 to 38 alter cellular resistance to HU and MMS. (A) *ubc9-10 top1*Δ cells transformed with reciprocal N-terminal y/hUbc9 chimeras, in YCpGAL1 vectors, were spotted onto selective galactose medium plus HU or MMS and incubated at 26°C or 36°C. (B) Overlay of ribbon diagrams of yeast (green) and human (magenta) Ubc9, rotated 180° around the *y* axis from the view in Fig. 4B, and close-up solid bond representations of residues $M_1(S_3)$ to F_{22} and F_{22} to L_{38} to emphasis differences in side chains. (C and D) Immunoblots of *ubc9-10 top1*Δ cells expressing the indicated *UBC9* allele at 36°C, stained with anti-Ubc9 (α Ubc9) (C) or α Smt3 (D) antibodies. *, nonspecific bands mirrored tubulin controls.

phenotypes induced by overexpression of a yeast E3 ligase or by reciprocal swaps of y/hUbc9 N-terminal domains.

SIZ1 encodes a PIAS family E3 ligase that directly interacts with Ubc9 and its targets to facilitate substrate SUMOylation (18). Other PIAS E3 ligases in yeast include Siz2 and Mms21 (18, 47). *SIZ1* and *SIZ2* are nonessential genes implicated in SUMO conjugation of septins and DNA topoisomerase II, while *MMS21* is an essential gene that regulates cell sensitivity to a wide range of DNA-damaging agents (18, 39, 47). In our hands, increased expression of *MMS21* or *SIZ2* genes failed to restore *ubc9-10* cell resistance to HU or Top1 poisons at 36°C (data not shown). In contrast, increased gene dosage of *SIZ1* on a multicopy vector restored *ubc9-10* cell resistance to the DNA damage induced by $Top1T_{722}A$ (Fig. 7A). Yet, increased levels of *SIZ1* failed to stabilize the $Ubc9P_{123}L$ protein or to restore global SUMO conjugates at 36°C (Fig. 7B). Moreover, the activity of Siz1 appeared to be specific for Top1-induced toxicity, as YEpSIZ1 failed to restore *ubc9-10* cell resistance to HU and decreased the low level of HU resistance conferred by overexpression of hUbc9 (Fig. 7C). In these experiments, hUbc9 was constitutively overexpressed, rather than expressed from the galactose-inducible promoter as in Fig. 2 and 3.

By contrast, results obtained with reciprocal N-terminal y/hUbc9 chimeras were quite surprising. As shown in Fig. 8A, the introduction of human residues 1 to 22 into yUbc9 (h_{22}yUbc9) had little effect on yUbc9 activity in suppressing *ubc9-10* sensitivity to HU or MMS. However, extending the chimeric junction to human residue 38 (h_{38}yUbc9) completely abrogated cell resistance to either agent. These data suggest that, in the context of hUbc9, yeast residues 22 to 38 provide determinants that are sufficient to dictate cell resistance to genotoxic stresses. In hUbc9, this spans β-sheet residues V_{25} and V_{27}, which are implicated by structural and mutational analyses to interact with hydrophobic residues in the RanBP2 E3 ligase (35, 40). Indeed, as highlighted in Fig. 8B, the presence of Y_{25} and K_{27} in yUbc9 would abrogate this hydrophobic surface, possibly dictating yeast SUMO E2/E3 interactions that are distinct from those observed with hUbc9 and RanBP2. On

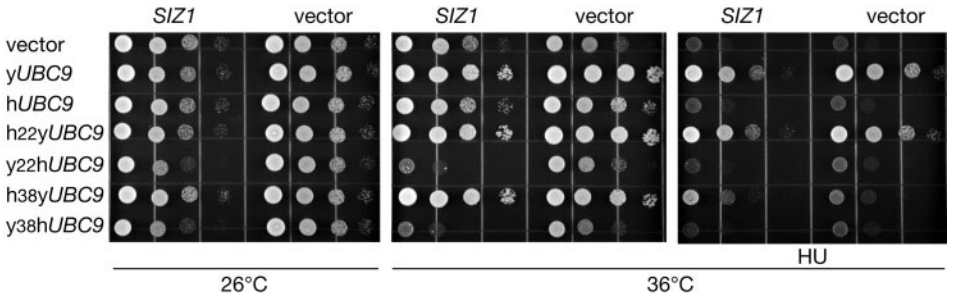

FIG. 9. Increased dosage of the Siz1 E3 ligase enhances the growth defects of y/h N-terminal Ubc9 chimeras. *ubc9-10 top1*Δ cells, cotransformed with YEpSIZ1 and YCpGAL1-UBC9 vectors, were spotted onto selective galactose plates with or without HU and incubated at 26°C or 36°C.

the other hand, introducing yeast N-terminal residues 1 to 22 into hUbc9 (either in y_{22}hUbc9 or y_{38}hUbc9p) exacerbated the slow-growth phenotype of *ubc9-10* cells at 36°C (Fig. 8A). These phenotypes could not be attributed to alterations in Ubc9 protein levels. The growth-inhibitory y_{22}hUbc9 and y_{38}hUbc9 proteins were expressed at high levels, while h_{22}yUbc9, which sufficed to restore *ubc9-10* cell growth and resistance to genotoxic stress at 36°C, was not detectable in immunoblots (Fig. 8C). As in Fig. 3, the introduction of N-terminal human residues precluded immunodetection of Ubc9. However, in this case, there was also a complete disconnect between detectable Ubc9 protein and cell viability. Rather, these data suggest that yeast residues 1 to 22 play a critical role in mediating Ubc9 interactions with yE1 and/or Smt3, while residues 22 to 38 modulate SUMO E2-E3 interactions to facilitate rather than dictate E2 substrate SUMOylation.

One prediction of this model is that yeast residues 1 to 22, in the context of hUbc9, would sequester yE1/Smt3 from interactions with endogenous yUbc9, effectively suppressing yUbc9 SUMO conjugation. Indeed, substantially lower levels of SUMO conjugates were detected in *ubc9-10* cells expressing y_{22}hUbc9 than in the vector control or cells expressing hUbc9 (Fig. 8D). A second prediction is that independent of the hUbc9 catalytic mechanism, inclusion of yeast residues 123 to 143 would complement the growth defect imposed by the N-terminal yeast residues by restoring appropriate substrate SUMOylation. Indeed, as seen in Fig. 8A and D, hUbc9 bearing yeast N-terminal residues (1 to 22 or 1 to 38) plus yeast residues 123 to 143 supported robust cell growth at 36°C, restored cellular resistance to HU and MMS, and, as shown for $y_{22}h_{123}y_{143}$hUbc9, restored global levels of SUMO conjugates.

A third prediction is that increasing substrate interactions with hUbc9 chimeras containing yeast N-terminal sequences, via elevated levels of an E3 ligase, would enhance the growth defects induced by E1/Smt3 sequestration by y_{22}hUbc9 or y_{38}hUbc9. As seen in Fig. 9, increased dosage of the Siz1 E3 ligase, sufficient to increase *ubc9-10* cell resistance to Top1 poisons (Fig. 7A), did enhance the cytotoxicity of y_{22}hUbc9 and y_{38}hUbc9. In contrast, YEpSIZ1 failed to alter the pattern of *ubc9-10* cell sensitivity to HU induced by expression of any of the N-terminal chimeras. Similar results were obtained with increased *SIZ2* gene dosage (data not shown). As these SUMO E3 ligases directly interact with select Ubc9 substrates, these findings support the premise that E1/Smt3 interactions with Ubc9, in concert with alterations in substrate binding, have distinct effects on cell viability and cellular responses to different genotoxic stresses.

DISCUSSION

Substrate specificity determinants of SUMO conjugation are of considerable interest, especially given the large number of target proteins, the complexity of E3 ligase activities, and the persistent alterations in protein function that are often imparted by comparatively transient SUMO modification (6, 12, 16, 24). In addition, Ubc9 appears to be unique among E2 conjugating enzymes in supporting SUMO conjugation in vitro in the absence of an E3 ligase. Structural studies demonstrate the interaction of conserved hUbc9 residues with the consensus ΨKX(D/E) motif in RanGAP1 (2). Moreover, the E3 ligase domain of RanBP2 interacts with hUbc9 and SUMO to facilitate thioester bond formation, rather then directly interacting with RanGAP1 (35, 40). Although substrate or E3 ligase binding by Ubc9 contributes to efficient SUMOylation, the role that the SUMO E2 plays in discriminating between substrates has remained unclear.

We previously reported that substitution of Leu for Pro_{123} in yeast Ubc9P_{123}L induced a synthetic lethal phenotype, whereby a global reduction in SUMO conjugates at 36°C sufficed to sustain cell viability yet enhanced cell sensitivity to a wide range of DNA-damaging agents. Thus, alterations in select target SUMOylation, induced by a single amino acid substitution in Ubc9, had an adverse impact on cell survival, but only in the context of genotoxic stress. Here we defined the functional domains in Ubc9 that dictate cellular responses to DNA-damaging agents versus those necessary to maintain cell viability in the absence of genotoxic stress, by assessing the biological consequences of subtle structural alterations in SUMO E2 activity.

A comparison of yeast and human Ubc9 activity in isogenic yeast strains and in in vitro SUMOylation assays illustrated distinct functional interactions of these highly conserved SUMO E2 enzymes. For instance, a 100-fold excess of yE1 was required to achieve Ubc9-Smt3 and Smt3-Smt3 conjugates with hUbc9 that were comparable to those with yUbc9, and hUbc9 was not as efficient a substrate for SUMOylation as yUbc9 (Fig. 1C). Recent biochemical studies demonstrated that Smt3 was efficiently activated and conjugated to human E1 in vitro (21). However, as the transfer of Smt3 to hUbc9 or yUbc9 was defective, those authors considered that surfaces

within the E1-SUMO thioester adduct provide some determinants for E2-thioester adduct formation. Our findings suggest that Ubc9 also provides determinants of E2 thioester transfer and that the differences between yeast and human Ubc9 proteins could be exploited to define differences in biological function.

Consistent with this premise, the slow-growth phenotype of *ubc9*Δ cells expressing hUbc9 was suppressed by the addition of C-terminal Myc or Flag tags, possibly as a consequence of increased protein stability or more efficient interactions with other components of the yeast SUMO pathway. Moreover, we found that N- or C-terminal modifications of hUbc9, sufficient to allow protein detection in immunoblots, also affected hUbc9 activity in yeast. In the structure of the SUMO-RanGAP1-Ubc9-RanBP2 complex, RanBP2 E3 ligase interactions span the C and N termini of hUbc9 (35, 40). Thus, it is tempting to speculate that similar interactions with an, as-yet-unidentified, yeast SUMO E3 could bridge N and C termini of Ubc9 to affect E2 function.

Structure/function of Ubc9. We also solved the structure of yUbc9, which in comparison with known structures of hUbc9 showed a considerable conservation of backbone architecture. The P_{123} residue, mutated in yUbc9P_{123}L and hUbc9P_{123}L, occupies the same position in both enzymes. Hydrogen-bonding interactions between the E2 side chain of N_{85} with backbone atoms of E2 residue N_{124} and the C-terminal SUMO-1 G_{97} residue within the E2 active site were revealed in the cocrystal structure of hUbc9 in complex with SUMO-1 conjugated to RanGAP1 (35). As these residues are conserved in yUbc9 and Smt3, such interactions are consistent with biochemical data indicating a role for N_{85} in stabilizing the transition state during E2 catalysis (45). We previously showed that substitution of Ala for Pro_{123} had no effect on yUbc9 function in vivo, while the introduction of the bulky hydrophobic side chain of Leu at this position reduced global SUMO conjugation and enhanced cell sensitivity to DNA damage at 36°C (15). Such a structural distortion in the $P_{123}N_{124}$ loop might compromise E2 catalysis by disrupting the coordination of N_{85} within the active site. We think this unlikely, however, as both yUbc9P_{123}L and hUbc9P_{123}L proteins were able to maintain *ubc9*Δ cell viability and were active in vitro (Fig. 2 and 3 and data not shown). Alternatively, binding of the extended Smt3 C terminus might suppress structural distortions induced by a temperature shift to 36°C.

Another possibility is that alterations in the geometry of the $P_{123}N_{124}$ loop might affect substrate binding by more distal C-terminal Ubc9 residues, such as residues 131 to 143. These largely nonconserved residues comprise helix C (Fig. 4B), which interacts with residues in RanGAP1 that flank the consensus ΨKXE site in cocrystal structures with hUbc9 (2, 35). Bernier-Villamor et al., (2) reported that mutation of several of these hUbc9 residues (A_{131} and Y_{134}) abolished efficient SUMOylation of RanGAP1 in vitro yet had limited effects on SUMO modification of two other substrates, p53 and IκBα. Thus, interactions of residues in RanGAP1 with helix C residues in hUbc9, required for efficient substrate modification, appeared to be substrate specific and, as such, were posited to provide binding surfaces for Ubc9 that could substitute for an E3 ligase. These considerations prompted the construction of yeast/human chimeras to determine whether such differences in side chain geometry would distinguish substrate SUMOylation necessary for cellular resistance to distinct genotoxic stresses and/or cell viability.

Indeed, differences in the geometries and charges of divergent side chains defined three determinants of Ubc9 activity in suppressing cell sensitivity to DNA-damaging agents, as follows.

(i) Ubc9 residues 123 to 143, implicated in binding of nonconserved residues within substrates that flank the SUMO consensus site. As mutation of human residues I_{125} and Q_{126} to match the P_{125} and N_{126} residues found in yUbc9 did not affect enzyme activity in vivo (data not shown), these findings support a model whereby residues 131 to 143 in helix C dictate select substrate interactions, while residues 123 to 130 contribute to the recognition of consensus SUMO site residues in substrate proteins.

(ii) Ubc9 residues 22 to 38, which interact with human RanBP2 E3 ligase. These data support a model whereby Ubc9 interactions with an E3 ligase, other than Siz1 or Siz2, facilitate substrate SUMOylation necessary to confer resistance to MMS and HU. This contrasts with the ability of Siz1 to act as a dosage suppressor of Top1-induced DNA damage. This model does not exclude additional interactions between Ubc9 residues 22 to 38 and SUMO E1, as suggested by the structure of Ubc12 and the E2 binding domain of NEDD8 E1 (14), although E1 and E3 binding to this Ubc9 domain may be mutually exclusive, as reported for other Ubl E2-E3 protein pairs (7).

(iii) N-terminal Ubc9 residues implicated in the binding of E1 and SUMO. Moreover, these studies demonstrate a functional interaction between N-terminal and substrate-binding domains of Ubc9 and support a model whereby chimeras that contain the N-terminal domain of yUbc9 and the substrate-binding determinants of hUbc9 act as dominant negative mutants by sequestering yE1/Smt3 to reduce global SUMOylation. This effect was exacerbated by increased dosage of Siz1 or Siz2 E3 ligase. However, this defect in Ubc9 activity was completely suppressed by introducing yUbc9 substrate-binding residues (123 to 143) into the same N-terminal chimeras. Thus, the introduction of yUbc9 residues implicated in E1/Smt3 binding (residues 1 to 22) and substrate binding (residues 123 to 143) redirects the catalytic activity of hUbc9 to maintain cell viability and restore cellular resistance to genotoxic stress.

In contrast, increased dosage of Siz1 E3 ligase (but not Siz2) partially suppressed *ubc9-10* cell sensitivity to Top1 poisons, with no effect on cell sensitivity to HU or MMS. Moreover, the extent of global SUMOylation supported by distinct E2 enzymes did not predict cellular resistance to genotoxic stress. Rather, our findings indicate that select substrate SUMOylation, dictated by specific E2/E3 interactions, distinguishes cellular resistance to distinct genotoxic stresses and provide a compelling rationale for developing novel chemotherapeutics that target specific components of the SUMO conjugation pathway.

ACKNOWLEDGMENTS

We thank Helen Walden, Andrew Larkin, and Padma Thimmaiah for their assistance, members of the Bjornsti and Schulman labs for helpful discussion, and staff at the X25 beamline at the National Synchrotron Light Source, Brookhaven National Laboratory.

This work was supported in part by NIH grants CA23099 and CA111542 (to M.-A.B.); the Pew Scholars Program, Beckman Young Investigator Award, Howard Hughes Medical Institute, and NIH grant GM069530 (to B.A.S.); an American Cancer Society fellowship (to D.M.D.); NCI Cancer Center core grant CA21765; and the American Lebanese Syrian Associate Charities.

REFERENCES

1. **Bencsath, K. P., M. S. Podgorski, V. R. Pagala, C. A. Slaughter, and B. A. Schulman.** 2002. Identification of a multifunctional binding site on Ubc9p required for Smt3p conjugation. J. Biol. Chem. **277:**47938–47945.
2. **Bernier-Villamor, V., D. A. Sampson, M. J. Matunis, and C. D. Lima.** 2002. Structural basis for E2-mediated SUMO conjugation revealed by a complex between ubiquitin-conjugating enzyme Ubc9 and RanGAP1. Cell **108:**345–356.
3. **Brunger, A. T., P. D. Adams, G. M. Clore, W. L. DeLano, P. Gros, R. W. Grosse-Kunstleve, J. S. Jiang, J. Kuszewski, M. Nilges, N. S. Pannu, R. J. Read, L. M. Rice, T. Simonson, and G. L. Warren.** 1998. Crystallography & NMR system: a new software suite for macromolecular structure determination. Acta Crystallogr. D **54:**905–921.
4. **Champoux, J. J.** 2001. DNA topoisomerases: structure, function, and mechanism. Annu. Rev. Biochem. **70:**369–413.
5. **Denison, C., A. D. Rudner, S. A. Gerber, C. E. Bakalarski, D. Moazed, and S. P. Gygi.** 2005. A proteomic strategy for gaining insights into protein sumoylation in yeast. Mol. Cell Proteomics **4:**246–254.
6. **Dohmen, R. J.** 2004. SUMO protein modification. Biochim. Biophys. Acta **1695:**113–131.
7. **Eletr, Z. M., D. T. Huang, D. M. Duda, B. A. Schulman, and B. Kuhlman.** 2005. E2 conjugating enzymes must disengage from their E1 enzymes before E3-dependent ubiquitin and ubiquitin-like transfer. Nat. Struct. Mol. Biol. **12:**933–934.
8. **Fiorani, P., and M. A. Bjornsti.** 2000. Mechanisms of DNA topoisomerase I-induced cell killing in the yeast Saccharomyces cerevisiae. Ann. N. Y. Acad. Sci. **922:**65–75.
9. **Fiorani, P., R. J. Reid, A. Schepis, H. R. Jacquiau, H. Guo, P. Thimmaiah, P. Benedetti, and M. A. Bjornsti.** 2004. The deubiquitinating enzyme Doa4p protects cells from DNA topoisomerase I poisons. J. Biol. Chem. **279:**21271–21281.
10. **Gill, G.** 2005. Something about SUMO inhibits transcription. Curr. Opin. Genet. Dev.
11. **Hannich, J. T., A. Lewis, M. B. Kroetz, S. J. Li, H. Heide, A. Emili, and M. Hochstrasser.** 2005. Defining the SUMO-modified proteome by multiple approaches in Saccharomyces cerevisiae. J. Biol. Chem. **280:**4102–4110.
12. **Hay, R. T.** 2005. SUMO: a history of modification. Mol. Cell **18:**1–12.
13. **Hayashi, T., M. Seki, D. Maeda, W. Wang, Y. Kawabe, T. Seki, H. Saitoh, T. Fukagawa, H. Yagi, and T. Enomoto.** 2002. Ubc9 is essential for viability of higher eukaryotic cells. Exp. Cell Res. **280:**212–221.
14. **Huang, D. T., A. Paydar, M. Zhuang, M. B. Waddell, J. M. Holton, and B. A. Schulman.** 2005. Structural basis for recruitment of Ubc12 by an E2 binding domain in NEDD8's E1. Mol. Cell **17:**341–350.
15. **Jacquiau, H. R., R. C. van Waardenburg, R. J. Reid, M. H. Woo, H. Guo, E. S. Johnson, and M. A. Bjornsti.** 2005. Defects in SUMO (small ubiquitin-related modifier) conjugation and deconjugation alter cell sensitivity to DNA topoisomerase I-induced DNA damage. J. Biol. Chem. **280:**23566–23575.
16. **Johnson, E. S.** 2004. Protein modification by SUMO. Annu. Rev. Biochem. **73:**355–382.
17. **Johnson, E. S., and G. Blobel.** 1999. Cell cycle-regulated attachment of the ubiquitin-related protein SUMO to the yeast septins. J. Cell Biol. **147:**981–994.
18. **Johnson, E. S., and A. A. Gupta.** 2001. An E3-like factor that promotes SUMO conjugation to the yeast septins. Cell **106:**735–744.
19. **Jones, T. A., J. Y. Zou, S. W. Cowan, and Kjeldgaard.** 1991. Improved methods for building protein models in electron density maps and the location of errors in these models. Acta Crystallogr. A **47:**110–119.
20. **Laskowski, R. A., M. W. MacArthur, D. S. Moss, and J. M. Thornton.** 1993. PROCHECK: a program to check the stereochemical quality of protein structures. J. Appl. Crystallogr. **26:**283–291.
21. **Lois, L. M., and C. D. Lima.** 2005. Structures of the SUMO E1 provide mechanistic insights into SUMO activation and E2 recruitment to E1. EMBO J. **24:**439–451.
22. **Maeda, D., M. Seki, F. Onoda, D. Branzei, Y. Kawabe, and T. Enomoto.** 2004. Ubc9 is required for damage-tolerance and damage-induced interchromosomal homologous recombination in S. cerevisiae. DNA Repair **3:**335–341.
23. **Megonigal, M. D., J. Fertala, and M. A. Bjornsti.** 1997. Alterations in the catalytic activity of yeast DNA topoisomerase I result in cell cycle arrest and cell death. J. Biol. Chem. **272:**12801–12808.
24. **Melchior, F., M. Schergaut, and A. Pichler.** 2003. SUMO: ligases, isopeptidases and nuclear pores. Trends Biochem. Sci. **28:**612–618.
25. **Nacerddine, K., F. Lehembre, M. Bhaumik, J. Artus, M. Cohen-Tannoudji, C. Babinet, P. P. Pandolfi, and A. Dejean.** 2005. The SUMO pathway is essential for nuclear integrity and chromosome segregation in mice. Dev. Cell **9:**769–779.
26. **Navaza, J.** 2001. Implementation of molecular replacement in AMoRe. Acta Crystallogr. D **57:**1367–1372.
27. **Otwinowski, A., and W. Minor.** 1997. Processing of X-ray diffraction data collected in oscillation mode. Methods Enzymol. **276:**307–326.
28. **Panse, V. G., U. Hardeland, T. Werner, B. Kuster, and E. Hurt.** 2004. A proteome-wide approach identifies sumoylated substrate proteins in yeast. J. Biol. Chem. **279:**41346–41351.
29. **Papa, F. R., A. Y. Amerik, and M. Hochstrasser.** 1999. Interaction of the Doa4 deubiquitinating enzyme with the yeast 26S proteasome. Mol. Biol. Cell **10:**741–756.
30. **Pfander, B., G. L. Moldovan, M. Sacher, C. Hoege, and S. Jentsch.** 2005. SUMO-modified PCNA recruits Srs2 to prevent recombination during S phase. Nature **436:**428–433.
31. **Pichler, A., P. Knipscheer, H. Saitoh, T. K. Sixma, and F. Melchior.** 2004. The RanBP2 SUMO E3 ligase is neither HECT- nor RING-type. Nat. Struct. Mol. Biol. **11:**984–991.
32. **Pommier, Y.** 2004. Camptothecins and topoisomerase I: a foot in the door. Targeting the genome beyond topoisomerase I with camptothecins and novel anticancer drugs: importance of DNA replication, repair and cell cycle checkpoints. Curr. Med. Chem. Anti-Cancer Agents **4:**429–434.
33. **Reid, R. J., P. Fiorani, M. Sugawara, and M. A. Bjornsti.** 1999. CDC45 and DPB11 are required for processive DNA replication and resistance to DNA topoisomerase I-mediated DNA damage. Proc. Natl. Acad. Sci. USA **96:**11440–11445.
34. **Reid, R. J., E. A. Kauh, and M. A. Bjornsti.** 1997. Camptothecin sensitivity is mediated by the pleiotropic drug resistance network in yeast. J. Biol. Chem. **272:**12091–12099.
35. **Reverter, D., and C. D. Lima.** 2005. Insights into E3 ligase activity revealed by a SUMO-RanGAP1-Ubc9-Nup358 complex. Nature **435:**687–692.
36. **Rodriguez, M. S., C. Dargemont, and R. T. Hay.** 2001. SUMO-1 conjugation in vivo requires both a consensus modification motif and nuclear targeting. J. Biol. Chem. **276:**12654–12659.
37. **Rosas-Acosta, G., W. K. Russell, A. Deyrieux, D. H. Russell, and V. G. Wilson.** 2005. A universal strategy for proteomic studies of SUMO and other ubiquitin-like modifiers. Mol. Cell Proteomics **4:**56–72.
38. **Seufert, W., B. Futcher, and S. Jentsch.** 1995. Role of a ubiquitin-conjugating enzyme in degradation of S- and M-phase cyclins. Nature **373:**78–81.
39. **Takahashi, Y., V. Yong-Gonzalez, Y. Kikuchi, and A. Strunnikov.** 2005. SIZ1/SIZ2 control of chromosome transmission fidelity is mediated by the sumoylation of topoisomerase II. Genetics **172:**783–794.
40. **Tatham, M. H., S. Kim, E. Jaffray, J. Song, Y. Chen, and R. T. Hay.** 2005. Unique binding interactions among Ubc9, SUMO and RanBP2 reveal a mechanism for SUMO paralog selection. Nat. Struct. Mol. Biol. **12:**67–74.
41. **Tong, H., G. Hateboer, A. Perrakis, R. Bernards, and T. K. Sixma.** 1997. Crystal structure of murine/human Ubc9 provides insight into the variability of the ubiquitin-conjugating system. J. Biol. Chem. **272:**21381–21387.
42. **Ulrich, H. D.** 2005. SUMO modification: wrestling with protein conformation. Curr. Biol. **15:**R257–R259.
43. **Vertegaal, A. C., S. C. Ogg, E. Jaffray, M. S. Rodriguez, R. T. Hay, J. S. Andersen, M. Mann, and A. I. Lamond.** 2004. A proteomic study of SUMO-2 target proteins. J. Biol. Chem. **279:**33791–33798.
44. **Wohlschlegel, J. A., E. S. Johnson, S. I. Reed, and J. R. Yates III.** 2004. Global analysis of protein sumoylation in Saccharomyces cerevisiae. J. Biol. Chem. **279:**45662–45668.
45. **Wu, P. Y., M. Hanlon, M. Eddins, C. Tsui, R. S. Rogers, J. P. Jensen, M. J. Matunis, A. M. Weisman, C. P. Wolberger, and C. M. Pickart.** 2003. A conserved catalytic residue in the ubiquitin-conjugating enzyme family. EMBO J. **22:**5241–5250.
46. **Yasugi, T., and P. M. Howley.** 1996. Identification of the structural and functional human homolog of the yeast ubiquitin conjugating enzyme UBC9. Nucleic Acids Res. **24:**2005–2010.
47. **Zhao, X., and G. Blobel.** 2005. A SUMO ligase is part of a nuclear multiprotein complex that affects DNA repair and chromosomal organization. Proc. Natl. Acad. Sci. USA **102:**4777–4782.
48. **Zhou, F., Y. Xue, H. Lu, G. Chen, and X. Yao.** 2005. A genome-wide analysis of sumoylation-related biological processes and functions in human nucleus. FEBS Lett. **579:**3369–3375.